mathematics

MDPI

Article

An Enhanced Smith-Predictor-Based Control Law for a MIMO CSTR with Multiple Time Delays †

Morteza Mohammadzaheri [1,*], Ali Al-Humairi [1], Gholamreza Vakili-Nezhaad [2], Aydin Azizi [3,*], Mojtaba Ghodsi [4] and Payam Soltani [5]

1 Faculty of Engineering and Computer Sciences, German University of Technology in Oman, GUTech Main Building, Halban 130, Oman; ali.alhumairi@gutech.edu.om
2 Engineering College, Sultan Qaboos University, Al Khodh 123, Oman; vakili@squ.edu.om
3 School of Engineering, Computing and Mathematics, Oxford Brookes University, Headington Campus, Oxford OX3 0BP, UK
4 School of Electrical and Mechanical Engineering, University of Portsmouth, Portsmouth PO1 3DJ, UK; mojtaba.ghodsi@port.ac.uk
5 System Engineering Department, Military Technological College, Al Matar Street, Muscat 111, Oman; payam.soltani@mtc.edu.om
* Correspondence: morteza.zaheri@gutech.edu.om (M.M.); aydin.azizi@brookes.ac.uk (A.A.)

† This paper is a revised and extended version of the authors' paper presented at the 28th IEEE International Conference on Automation and Computing, Birmingham, UK, 30 August–1 September 2023.

Abstract

This paper introduces an enhanced Smith-predictor-based control system (SPCS) for multi-input multi-output (MIMO) time delay processes. A conventional SPCS for an MIMO process is composed of a Smith predictor matrix providing predicted outputs and an array of classical feedback controllers. These controllers act on predicted error signals, calculated by subtracting the predicted output from the reference signal at the time of operation. Two major shortcomings were idented for the underperformance of conventional SPCSs for MIMO time-delay processes: (i) the employed classical feedback controllers are designed based on trade-off. Moreover, their use may lead to a windup phenomenon, which adversely influences the control performance of conventional SPCSs; (ii) a predicted output generated by a Smith predictor corresponds to a future time and is therefore not concurrent with the reference at the time of operation. Thus, in conventional SPCSs, the control error is generated using two asynchronous signals. This article proposes two enhancements to tackle the aforementioned dual shortcomings in SPCSs for MIMO time-delay systems. The proposed control system is shown to distinctly outperform a conventional SPCS with proportional-integral-derivative (PID) feedback controllers. The case study is a catalytic stirred tank reactor (CSTR) with three inputs (feed and water flow rates and auxiliary temperature), two outputs (output flow concentration and temperature) and three different time delays. The presented CSTR model, used for the design and simulations, is more comprehensive than any CSTR model reported in the literature.

Keywords: Smith predictor; time-delay system; CSTR; MIMO; feedforward; asynchrony

MSC: 93B45

Check for updates

Academic Editors: Jianhua Zhang, Weicun Zhang, Jing Na and Qiang Chen

Received: 24 July 2026
Revised: 3 September 2026
Accepted: 16 September 2026
Published: 20 September 2026

1. Introduction

Several dynamic systems exhibit dead time or time delay and are consequently classified as time-delay systems [1–5]. These include chemical processes, vibrational systems, engines, manufacturing and telecommunication systems, etc. [6–13]. Time delay is largely regarded as a source of instability and poor performance in control systems [14,15]. The control of time-delay systems, witnessing a significant time delay, should be differentiated from time-delay estimation (TDE) as a technique in control to estimate unknown/uncertain system dynamics and disturbances using delayed measurements for systems that may not witness a significant time delay [16].

There are two categories of time-delay systems, widely known as network-induced and input-delay [17]. Network-induced delay, also known as communication delay [18], is caused by the time required to exchange data between devices over electrical/communication networks. In this category, the states of a system affect their time derivatives with a delay. The control of systems with network-induced time delay is addressed using Lyapunov–Krasovskii and Razumikhin theorems [19,20] and is out of the scope of process control and this paper. On the other hand, in the input-delay category, the control inputs affect the time derivatives of the system states with a delay, i.e., the actuator(s) affect the system after a non-negligible time [21,22]. This category of time delay is a serious concern in process control [23,24] and is the focus of this paper.

Two main approaches have been employed to design model-based control systems for processes with input delay: (i) integrating the delay into the model prior to control system design and (ii) the use of predictors/predictive models. Recently, the first approach has been used in the discrete/digital domain, but only for electromechanical systems with very short ($<$10 ms) delays [25,26] and not yet for process control. Alternatively, the first approach has long been used in the continuous domain, where the term exhibiting the delay in the model (i.e., an exponential term in the Laplace domain) is replaced by its Pade approximate transfer function, an all-pass filter in the Laplace domain. This approximate transfer function is then integrated into the delay-free part of the model [24,27]. Subsequently, the resultant model is employed for control system design. Pade approximation results in model inaccuracy and converts a stable minimum-phase system to a non-minimum-phase one with a higher order [24]. These disadvantages, however, do not exist in the second approach or predictive methods, such as Smith predictors [28]. As a result, they are anticipated to exhibit higher performance.

Smith predictors were originally developed for stable SISO systems, but their application was later extended to MIMO systems with multiple delays [29,30], unstable systems [31], long delays [32] and disturbance [33]. Consequently, Smith predictors were proposed to be a part of control solution for any stable or unstable time-delay system [21,34] and even branded as the "best approach to deal with time delays" [35].

However, a drawback recently emerged in SPCSs: despite all the mentioned advantages and advances of SPCSs, some research works demonstrated that feedback-control systems based on Pade approximation outperform SPCSs, for example in the control of linear systems with identifiable time-varying delays [36,37]. In response, design shortcomings leading to such an unexpected underperformance of SPCSs were identified for single-input single-output (SISO) systems in [17], and an enhanced SPCS, with improved performance, was introduced, detailed in Section 2. The proposed method was, however, never extended to MIMO systems. Also, no work in the literature was found by the authors addressing or even recognizing the mentioned shortcomings in SPCSs designed for MIMO systems. The paper fills this research gap and extends the enhanced SPCS to MIMO systems as its main technical novelty. The case study of this paper is the full-scale tracking control of a CSTR with three inputs, two outputs and three time delays. The employed CSTR model is unprecedented in its inclusion of system details, to the best of the authors' knowledge, as detailed in the first paragraph of Section 4.

This paper continues with an introduction to the enhanced SPCS for SISO systems in Section 2, followed by the newly developed enhanced SPCS for MIMO systems, which is the main methodology section of the paper, described in Section 3. Section 4 introduces the case study, simultaneous affluent concentration and temperature control in an exothermic nonlinear CSTR with three inputs and all possible time delays. This section includes a stability analysis specific to the presented case study. Section 5 presents the results and demonstrates how the proposed methodology led to the improvement in control behaviour. The paper is concluded by Section 6.

2. Enhanced SISO Smith-Predictor-Based Control Systems—A Brief Review

Figure 1 shows a generic SISO SPCS, where $G(s)$ and $\hat{G}(s)$ are the plant true and approximated transfer functions without the delay, respectively:

$$y(s) = u(s)\, e^{-st_1} G(s), \tag{1}$$

where t_1 is the time delay in a time unit, and e^{-st_1} represents the delay in the Laplace domain. u, y and y_d are the input, output and its reference. In Figures 1–3, $C(s)$ is a linear classical controller designed for G(s), and hat ˆ indicates an approximation.

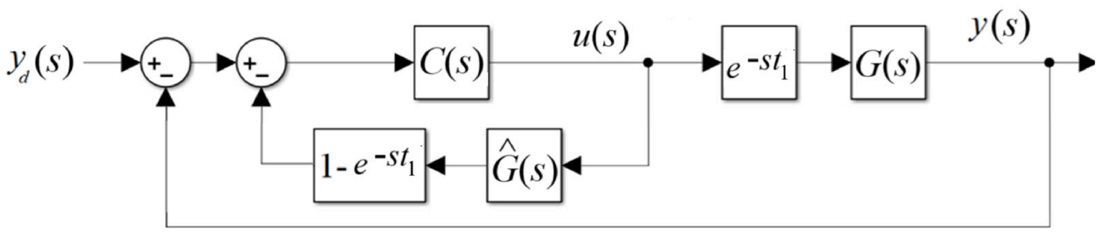

Figure 1. Schematics of a conventional Smith-predictor-based control system in Laplace domain.

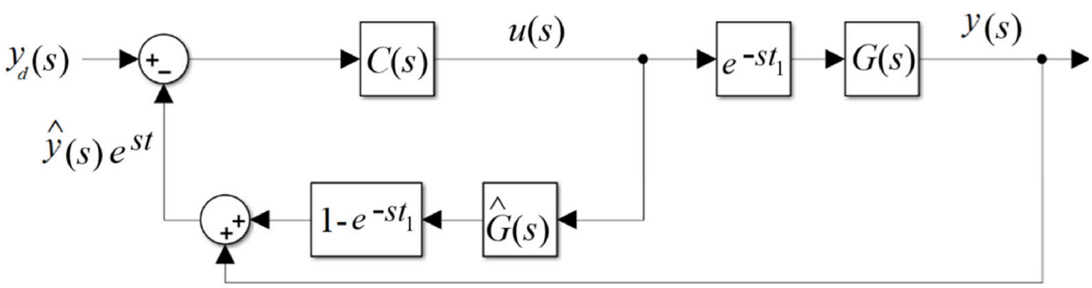

Figure 2. A re-arranged presentation of Figure 1.

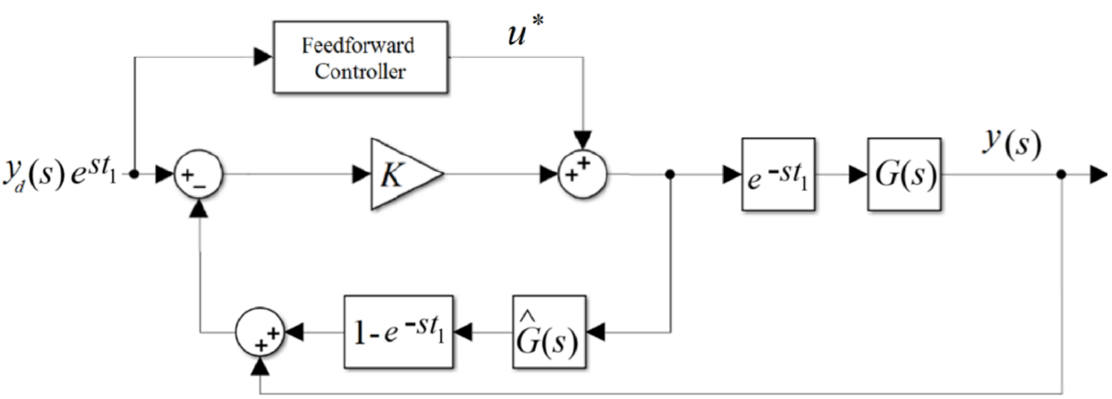

Figure 3. An enhanced Smith-predictor-based control system for a SISO problem.

Figure 2 is the re-arranged form of Figure 1. As mentioned earlier, the control architecture presented in Figure 1 has two inherent shortcomings: (i) the use of a classical feedback controller, $C(s)$, intrinsically designed based on trade-off, and (ii) the reference y_d is compared with the approximated output at a time in the future. Figure 2 clearly demonstrates the asynchrony between signals generating the error in a conventional SPCS.

Detailed analysis in [17] concludes that the architecture presented in Figure 3 eliminates both aforementioned shortcomings. If $G(s)$ is a first-order transfer function, K and u^* will be real numbers and stabilize the system [14]. $y_d\ (s)\ e^{st_1}$ is the future value of the reference t_1 time units ahead of the current time.

3. Enhanced MIMO Smith-Predictor-Based Control Systems

This section reports the development of an enhanced SPCS for linear MIMO time-delay processes, presented in Equation (2):

$$\begin{bmatrix} y_1(s) \\ \vdots \\ y_{n_y}(s) \end{bmatrix} = \begin{bmatrix} G_{11}(s)e^{-st_{11}} & \dots & G_{1n_u}(s)e^{-st_{1n_u}} \\ \vdots & \ddots & \vdots \\ G_{n_y1}(s)e^{-st_{n_y1}} & \dots & G_{n_yn_u}(s)e^{-st_{n_yn_u}} \end{bmatrix} \begin{bmatrix} u_1(s) \\ \vdots \\ u_n(s) \end{bmatrix}, \tag{2}$$

where n_u and n_y are the number of inputs and outputs, respectively, and t stands for time delay. As pioneers, Ogunnaike and Ray extended the original SPCS, based on classical controllers, to MIMO linear systems [38]. Their works led to a control law of Equation (3) for Equation (2):

$$u_j(s) = \sum_{i=1}^{n_y} C_{ij}(s)\left(y_{d_i}(s)\ -\ y_{p_i}(s)\right), \tag{3}$$

where all C_{ij} controllers are classical controllers, and indices p and d stand for predicted and desired. Either Equations (4) or (5) yield the predicted output components, y_{p_i}s:

$$y_{p_i}(s) = \sum_{j=1}^{n_u} \hat{G}_{ij}(s)u_j(s)\left(1\ -\ e^{-st_{ij}}\right) + y_i(s), \tag{4}$$

$$\begin{bmatrix} y_{p1}(s) \\ \vdots \\ y_{pn_y}(s) \end{bmatrix} = \overbrace{\begin{bmatrix} \hat{G}_{11}(s)\left(1-e^{-st_{11}}\right) & \dots & \hat{G}_{1n_u}(s)\left(1-e^{-st_{1n_u}}\right) \\ \vdots & \ddots & \vdots \\ \hat{G}_{n_y1}(z)\left(1-e^{-st_{n_y1}}\right) & \dots & \hat{G}_{n_yn_u}(z)\left(1-e^{-st_{n_yn_u}}\right) \end{bmatrix}}^{predictor\ matrix} \begin{bmatrix} u_1(s) \\ \vdots \\ u_{n_u}(s) \end{bmatrix} + \begin{bmatrix} y_1(s) \\ \vdots \\ y_{n_y}(s) \end{bmatrix}. \tag{5}$$

The use of an array of classical controllers, similar to $C_{ij}(s)$s in Equation (3), is still the dominant approach to SPCS for MIMO systems [39–41]. For the system of Equation (2) and the control law of Equation (3), ref. [38] showed that delays do not affect the closed loop stability, if the discrepancy of $G_{ij}(s)$ and $\hat{G}_{ij}(s)$ is negligible for all values of i and j. That is, if C_{ij} controllers can stabilize the delay-less system, they can stabilize Equation (2) too.

The control law of Equation (3), as a broadly accepted form of an MIMO SPCS, is of the following shortcomings similar to its SISO counterpart:

(i) Classical controllers of C_{ij} are subject to trade-off in design and/or windup. The design of classical controllers entails a trade-off between achieving satisfactory control performance and minimizing steady-state error. In addition, the windup phenomenon (the effect of actuator's saturation on integrals [42]) occurs in classical controllers. Both the trade-off-based design and windup (including anti-windup components) may adversely affect the control response and result in non-optimal behavior.

(ii) y_{pi} and y_{di} are asynchronous in Equation (3). In order to clarify this asynchrony, Equation (4) can be extended as follows:

$$y_{pi}(s) = \sum_{j=1}^{n_u} \hat{G}_{ij}(s)u_j(s)\left(1 - e^{-st_{ij}}\right) + \overbrace{\sum_{j=1}^{n_u} G_{ij}(s)u_j(s)e^{-st_{ij}}}^{y_i(s)} \overset{G_{ij}\approx\hat{G}_{ij}}{\Rightarrow} y_{pi}(s) \approx \sum_{j=1}^{n_u} \overbrace{\hat{G}_{ij}(s)u_j(s)}^{y_{pij}(s)} = \sum_{j=1}^{n_u} y_{pij}(s).$$

Therefore,

$$y_{pij}(s) = G_{ij}(s)u_j(s), \tag{6}$$

where y_{pij} is a constituent of y_{pi} influenced by u_j. Moreover, from Equation (2),

$$y_i(s) = \sum_{j=1}^{n_u} \overbrace{G_{ij}(s)u_j(s)e^{-st_{ij}}}^{y_{ij}(s)} = \sum_{j=1}^{n_u} y_{ij}(s) \Rightarrow y_{ij}(s) = G_{ij}(s)u_j(s)e^{-st_{ij}}, \tag{7}$$

where y_{ij} is the constituent of y_i influenced by u_j.

A comparison of Equations (6) and (7) shows that, in the conventional MIMO SPCS, demonstrated by Equations (3) and (4), the constituents of predicted output (y_{pij} s) are not of the same time as the constituents of the output, y_{ij}. In fact, y_{ij} is t_{ij} time units behind y_{pij}. Therefore, in the conventional MIMO SPCS, two asynchronous variables (y_{di} and y_{pi}) are compared to find the control error, fed to the controller.

In order to address the aforementioned dual shortcomings, two enhancements are proposed for SPCSs designed for MIMO time-delay systems. Enhancement 1 eliminates the need for classical feedback controllers (shortcoming 1), and Enhancement 2 addresses asynchrony (shortcoming 2).

<u>Enhancement 1 MIMO:</u> A feedback–feedforward control law of Equation (8) replaces the array of the feedback controller of C_{ij} s in Equation (3):

$$u_j = {u_j}^* + \sum_{\iota=1}^{n_x} K_{\iota j}\left(x_{d\iota} - x_{p\iota}\right), j = 1 : n_u, \tag{8}$$

where $K_{\iota j}$ is an element of $\mathbf{K}$ determined through pole placement. $x_{d\iota}$ and $x_{p\iota}$ are the states calculated based on y_{di} s and y_{pi} s. u^*_j is an input at the desired status.

Justification for Enhancement 1 MIMO: As in [38], providing that the discrepancy of G_{ij} and $\hat{G}_{ij}$ is negligible, a control system that stabilizes the delay-free process, i.e., Equation (2), when $\forall\ r_{ij} = 0$, also stabilizes the original time-delay process, i.e., Equation (2), with any values of r_{ij}. Let us assume that Equation (9) is a continuous state space model of the delay-free system:

$$\begin{cases} \dot{\mathbf{X}} = \mathbf{AX} + \mathbf{BU} \\ \mathbf{Y} = \mathbf{CX} \end{cases}. \tag{9}$$

With the desired status of Equation (10),

$$\begin{cases} \dot{\mathbf{X}}_d = \mathbf{AX}_d + \mathbf{BU}^* \\ \mathbf{Y}_d = \mathbf{CX}_d \end{cases}. \tag{10}$$

By subtracting Equation (9) from Equation (10),

$$\begin{cases} \dot{\mathbf{X}}_d - \dot{\mathbf{X}} = \mathbf{A}(\mathbf{X}_d - \mathbf{X}) + \mathbf{B}(\mathbf{U}^* - \mathbf{U}) \\ \mathbf{Y_d} - \mathbf{Y} = \mathbf{C}(\mathbf{X}_d - \mathbf{X}) \end{cases}. \tag{11}$$

A state vector feedback control law of Equation (12), designed to place stable poles for Equation (11), stabilizes Equation (9), the delay-free system [43].

$$\mathbf{U} = \mathbf{K}(\mathbf{X}_d - \mathbf{X}) + \mathbf{U}^*. \tag{12}$$

This pushes the error, $\mathbf{Y}_d - \mathbf{Y}$, towards zero. Equation (12) is an equivalent of Equation (8).

Enhancement 2 MIMO: $y_{di}\big(t + \max t_{ij} | j = 1 : n_u\big)$ is used to derive $x_{d\iota}$ and u_j for control law of Equation (8).

As explained in the shortcoming (ii), y_{ij} is t_{ij} time units behind y_{pij}, or y_{pi} is the predicted output for a future time. However, in conventional MIMO SPCSs, y_{pi} is compared with the present time reference, y_{di}, to produce the control error. Enhancement 2 addresses this issue with the use of future values of reference upfront to produce the control error. This enhancement is usable only when the reference trajectory is known in advance or the reference preview is possible. The reference preview, whereby future values of the reference trajectory are available to the controller, has been long used in control [44] and is widely applicable in process control [45].

4. Case Study, a MIMO CSTR

The case study is an exothermic continuous stirred tank reactor (CSTR) with two control outputs, three control inputs and three distinct delays. This system is modeled as Equation (13), composed of molar equilibrium and energy equilibrium equations. In fact, Equation (13) is the combination of a single-delay two-output model presented in [46] and a double-input model of [47]; it furthermore includes all possible time delays, overlooked in previous research. Two outputs of the CSTR model of Equation (13) are the effluent concentration $C_A(t)$ [mol/L] and temperature $T(t)$ [K]. The control inputs are the feed flow rate $q_f(t)$ [L/min], water flow rate $q_w(t)$ [L/min] and auxiliary temperature $T_x\ (t)$ [K]. θ_1, θ_2 and θ_3 [min] represent time delays.

$$\begin{cases} V\frac{dC_A(t)}{dt} = q_f(t-\theta_1)\Big(C_f - C_A(t)\Big) + q_w(t-\theta_1)(0 - C_A(t)) - V\kappa exp\Big(\frac{-E}{RT(t)}\Big)C_A(t), \\ V\rho c\frac{dT(t)}{dt} = \Big(q_f + q_w\Big)(t-\theta_2)\rho c\Big(T_f - T(t)\Big) - VH\kappa exp\Big(\frac{-E}{RT(t)}\Big)C_A(t) - U(T(t) - T_x(t-\theta_3)). \end{cases} \tag{13}$$

V, C_f, κ, E, R, c, U, H and ρ stand for the reactor volume [L], feed concentration [mol/L], reaction velocity constant [min^{-1}], Arrhenius activation energy [J/mol], gas constant [J/(mol.K)], specific heat capacitance [g/(L.K)], overall heat transfer coefficient [J/(min.K)], heat of reaction [J/min] and density [g/L], respectively. The water and feed temperature are assumed to be equal, T_f. All listed parameters are assumed to be time-invariant. In order to find the parameters of the control system of Equations (8) or (12), according to the methodology presented in Section 3, the system needs to be linearized first to match Equation (2) or its state space equivalent; then, feedback and feedforward controllers and the MIMO Smith predictor, as well as the maximum delays detailed in Enhancement 2, are identified, as detailed in Section 4.2.

4.1. Linearization of the Model

This subsection elucidates how Equation (13), with three inputs, is converted into dual models for control purposes, each with two inputs: (i) model Equation (14) when the concentration is intended to increase and (ii) model Equation (15) when the concentration is intended to decrease. These dual models were approximated using the linear state equations of Equations (16) and (17) for state vector feedback control system design.

Plausibly, feed and water valves, which are utilized to increase and decrease the concentration, should not function simultaneously. Therefore, two different models of

Equations (14) and (15) are proposed for situations where the concentration is intended to increase (water valve is closed) or to decrease (feed valve is closed), respectively:

$$\begin{cases} V\frac{dC_A(t)}{dt} = q_f(t-\theta_1)\Big(C_f - C_A(t)\Big) - V\kappa exp\Big(\frac{-E}{RT(t)}\Big)C_A(t), \\ V\rho c\frac{dT(t)}{dt} = q_f(t-\theta_2)\rho c\Big(T_f - T(t)\Big) - VH\kappa exp\Big(\frac{-E}{RT(t)}\Big)C_A(t) - U(T(t) - T_x(t-\theta_3)). \end{cases} \tag{14}$$

$$\begin{cases} V\frac{dC_A(t)}{dt} = -q_w(t-\theta_1)C_A(t) - V\kappa exp\Big(\frac{-E}{RT(t)}\Big)C_A(t), \\ V\rho c\frac{dT(t)}{dt} = q_w(t-\theta_2)\rho c\Big(T_f - T(t)\Big) - VH\kappa exp\Big(\frac{-E}{RT(t)}\Big)C_A(t) - U(T(t) - T_x(t-\theta_3)). \end{cases} \tag{15}$$

Compared to Equation (13), q_w and q_f equal zero in Equations (14) and (15), respectively.

Let us consider C_A, T, q_f, q_w and T_x as y_1, y_2, u_1, u_2 and u_3, respectively. With the use of nominal values of parameters listed in [46] and Table 1, as well as reasonable delays, Equations (14) and (15) are converted to Equations (16) and (17), respectively.

$$\begin{cases} \dot{y}_1(t) = u_1(t-0.05)(0.01 - 0.01y_1(t)) - 7.2\times 10^{10}exp\Big(\frac{-8750}{y_2(t)}\Big)y_1(t), \\ \dot{y}_2(t) = u_1(t-0.1)(3.5 - 0.01y_2(t)) + 1.506\times 10^{13}y_1(t)exp\Big(\frac{-8750}{y_2(t)}\Big) - 2.092(y_2(t) - u_3(t-0.2)). \end{cases} \tag{16}$$

$$\begin{cases} \dot{y}_1(t) = -u_2(t-0.05)(0.01y_1(t)) - 7.2\times 10^{10}exp\Big(\frac{-8750}{y_2(t)}\Big)y_1(t), \\ \dot{y}_2(t) = u_2(t-0.1)(3.5 - 0.01y_2(t)) + 1.506\times 10^{13}y_1(t)exp\Big(\frac{-8750}{y_2(t)}\Big) - 2.092(y_2(t) - u_3(t-0.2)). \end{cases} \tag{17}$$

Table 1. Nominal values of model parameters.

Parameter	Value	Parameter	Value
C_f	1 mol/L	H	5×10^4 J/min
T_f	350 K	E/R	8750 K
U	5×10^4 J/(min K)	κ	7.2×10^{10} 1/min
c	0.239 g/(L.K)	ρ	1000 g/L
V	100 L		

For control system design purposes, Equation (16) was linearized around the operating point of $\bar{y}_1 = 0.2$ mol/L and $\bar{y}_2 = 300$ K, to produce an approximate linear model when the concentration is intended to rise:

$$\begin{bmatrix} \dot{y}_1(t) \\ \dot{y}_2(t) \end{bmatrix} = \begin{bmatrix} -0.016 & 0 \\ 3.243 & -2.102 \end{bmatrix} \begin{bmatrix} y_1(t) \\ y_2(t) \end{bmatrix} + \begin{bmatrix} 0.008e^{-0.05s} & 0 \\ 0.500e^{-0.1s} & 2.092e^{-0.2s} \end{bmatrix} \begin{bmatrix} u_1(t) \\ u_3(t) \end{bmatrix}. \tag{18}$$

Similarly, if the concentration is intended to decline, the approximate linear model of Equation (17) is

$$\begin{bmatrix} \dot{y}_1(t) \\ \dot{y}_2(t) \end{bmatrix} = \begin{bmatrix} -0.016 & 0 \\ 3.243 & -2.102 \end{bmatrix} \begin{bmatrix} y_1(t) \\ y_2(t) \end{bmatrix} + \begin{bmatrix} -0.002e^{-0.05s} & 0 \\ 0.500e^{-0.1s} & 2.092e^{-0.2s} \end{bmatrix} \begin{bmatrix} u_2(t) \\ u_3(t) \end{bmatrix}. \tag{19}$$

All numbers in Equations (18) and (19) and future sections, which are the results of calculations, have been rounded to keep the paper concise. Numbers with a precision of 15 decimal digits were used in simulations.

4.2. Control

In this research, the proposed enhanced MIMO SPCS of Equation (8) was employed to simultaneously control the concentration and temperature in the presence of all possible time delays. The sole control of temperature [48] or concentration [46] has been reported for CSTRs in the presence of a time delay. However, none of several double-input double-output control solutions for CSTRs, e.g., [47,49–55], consider and address time-delay(s).

In order to develop the proposed enhanced SPCS, presented in Equation (8), the following should be defined:

(i) feedback control gains, K_{ij} s in Equation (8), which are the elements of **K** in Equation (12);
(ii) a feedforward control law defining u_j* in Equation (8), or practically u_1*, u_2* and u_3* in this problem;
(iii) Smith predictor to estimate $x_{p\iota}$ s in (8) or practically predicted y_1 and y_2 in this case study;
(iv) values of maximum t_{ij}, which are practically max (t_{11} and t_{12}) to be used with u_1, max (t_{21} and t_{22}) to be used with u_2 and max (t_{31} and t_{32}) to be used with u_3.

4.2.1. Feedback Control Gains

In the investigated case study, the states, represented by x in Equation (8), are the same as the outputs, represented by y. The delay-free form of state space models, Equations (18) and (19), were used to obtain feedback control gains. Closed loop poles of -5 and -2 were selected for the concentration and temperature, y_1 and y_2, respectively. The pole associated with the concentration was selected further from zero due to the higher importance of this output. The matrices of feedback control gains, when the concentration is intended to increase or decrease, are shown as **K** in Equations (20) and (21), respectively:

$$\begin{bmatrix} u_1 \\ u_3 \end{bmatrix} = \overbrace{\begin{bmatrix} 623.0622 & 0 \\ -147.3616 & -0.0488 \end{bmatrix}}^{\mathbf{K}} \begin{bmatrix} y_{d1} - y_1 \\ y_{d2} - y_2 \end{bmatrix} + \begin{bmatrix} u^*{}_1 \\ u^*{}_3 \end{bmatrix}. \tag{20}$$

$$\begin{bmatrix} u_2 \\ u_3 \end{bmatrix} = \overbrace{\begin{bmatrix} -2492.2486 & 0 \\ 597.1977 & -0.0488 \end{bmatrix}}^{\mathbf{K}} \begin{bmatrix} y_{d1} - y_1 \\ y_{d2} - y_2 \end{bmatrix} + \begin{bmatrix} u^*{}_2 \\ u^*{}_3 \end{bmatrix}. \tag{21}$$

4.2.2. Feedforward Control Law Regardless of Time Delays

At the desired status of $\dot{y}_1(t) = \dot{y}_2(t) = 0$, $y_1 = y_{d1}$ and $y_2 = y_{d2}$, the delay-free form of Equations (16) and (17) leads to Equations (22) and (23):

$$\begin{cases} 0 = u^*{}_1(0.01 - 0.01y_{d1}) - 7.2 \times 10^{10} y_{d1} exp\left(\frac{-8750}{y_{d2}}\right), \\ 0 = u^*{}_1(3.5 - 0.01y_{d2}) + 1.506 \times 10^{13} y_{d1} exp\left(\frac{-8750}{y_{d2}}\right) - 2.092(y_{d2} - u^*{}_3). \end{cases} \tag{22}$$

$$\begin{cases} 0 = -u^*{}_2(0.01y_{d1}) - 7.2 \times 10^{10} y_{d1} exp\left(\frac{-8750}{y_{d2}}\right), \\ 0 = u^*{}_2(3.5 - 0.01y_{d2}) + 1.506 \times 10^{13} y_{d1} exp\left(\frac{-8750}{y_{d2}}\right) - 2.092(y_{d2} - u^*{}_3). \end{cases} \tag{23}$$

The combination of the second equations in Equations (22) and (23) leads to Equation (24):

$$0 = 0.5(u^*{}_1 + u^*{}_2)(3.5 - 0.01y_{d2}) + 1.506 \times 10^{13} y_{d1} exp\left(\frac{-8750}{y_{d2}}\right) - 2.092(y_{d2} - u^*{}_3) \Rightarrow$$

$$u^*{}_3 = \frac{1}{-2.092}\left(0.5(u^*{}_1 + u^*{}_2)(3.5 - 0.01y_{d2}) + 1.506 \times 10^{13} y_{d1} exp\left(\frac{-8750}{y_{d2}}\right) - 2.092(y_{d2})\right). \tag{24}$$

The following feedforward control law is derived out of (22, 23 and 24):

$$\begin{cases} u^*{}_1 = y_{d1}\left(1 + 7.2 \times 10^{12} exp\left(\frac{-8750}{y_{d2}}\right)\right), \text{if concentration is set to increase, otherwise } 0 \\ u^*{}_2 = -7.2 \times 10^{12} exp\left(\frac{-8750}{y_{d2}}\right), \text{if concentration is set to decrease, otherwise } 0 \\ u^*{}_3 = -0.2390(u^*{}_1 + u^*{}_2)(3.5 - 0.01 y_{d2}) - 7.2 \times 10^{12} y_{d1} exp\left(\frac{-8750}{y_{d2}}\right) + y_{d2}. \end{cases} \quad (25)$$

4.2.3. Smith Predictor

Equations (18) and (19) can be converted to Equations (26) and (27) to produce G_{ij} (s) $e^{(-st_{ij})}s$ of Equation (7):

$$\begin{bmatrix} y_1(s) \\ y_2(s) \end{bmatrix} = \begin{bmatrix} \frac{0.008\ s\ +\ 0.0168}{s^2 +\ 2.118\ s\ +\ 0.0326} e^{-0.05s} & 0 \\ \frac{0.5\ s\ +\ 0.0337}{s^2 +\ 2.118\ s\ +\ 0.0326} e^{-0.1s} & \frac{2.092\ s\ +\ 0.0324}{s^2 +\ 2.118\ s\ +\ 0.0326} e^{-0.2s} \end{bmatrix} \begin{bmatrix} u_1(s) \\ u_3(s) \end{bmatrix}. \quad (26)$$

$$\begin{bmatrix} y_1(s) \\ y_2(s) \end{bmatrix} = \begin{bmatrix} \frac{-0.002\ s - 0.0042}{s^2 + 2.118\ s + 0.0326} e^{-0.05s} & 0 \\ \frac{0.5\ s + 0.0013}{s^2 + 2.118\ s + 0.0326} e^{-0.1s} & \frac{2.092\ s + 0.0324}{s^2 + 2.118\ s + 0.0326} e^{-0.2s} \end{bmatrix} \begin{bmatrix} u_2(s) \\ u_3(s) \end{bmatrix}. \quad (27)$$

4.2.4. Maximum t_{ij}

Equations (26) and (27) evidently show that max t_{1j} is 0.05 min and max t_{2j} is 0.2 min. With these delays, in the control law of Equation (8), $x_{d1} = y_{d1}(t + 0.05)$ and $x_{d2} = y_{d2}(t + 0.2)$. Consequently, in practice, $y_{d1}(t + 0.05)$ and $y_{d2}(t + 0.2)$ were used instead of y_{d1} and y_{d2} in Equations (20), (21) and (25).

4.2.5. Stability Remarks and Limitations

The provided methodology in Section 3 guarantees the stability of linear systems presented by Equation (2) or its state space equivalent. As detailed in the *Justification for Enhancement 1 MIMO* in Section 3, if the control system stabilizes the delay-free system and the models used in the Smith predictor are highly accurate, the same control system stabilizes the system with a time delay. The control law of Equation (12), also presented as Equation (8), designed based on pole placement, easily stabilizes the linear delay-free system, since closed loop poles with the negative real part are selected. However, the case study is originally nonlinear, and the provided control law can only guarantee the stability of its linearized approximate. This is an intrinsic limit of the provided methodology, which is aligned with the fact that Smith predictors are essentially developed for linear systems. This suggests that SPCS as a whole, including its proposed enhanced version, is an undesirable choice for highly nonlinear systems.

However, for the case study and most processes, bounded-input bounded-output (BIBO) stability can be demonstrated. In the case study presented in the paper, i.e., Equation (13), also presented in Equations (16) and (17), y_1 or the affluent concentration is evidently bounded. The following corollary shows, with a reference of $y_{d2} = 350$ K, that the affluent temperature stops increasing after it reaches the reference, when the concentration is intended to rise; 350 K is the maximum temperature of auxiliary flow in this case study, which is the highest meaningful reference of the affluent temperature, y_2 [56]. Since the initial temperature value is plausibly below 350 K, the use of 350 K as the highest reference of y_2 is expected to lead to the largest error values and most severe control actions to increase the temperature. The corollary shows, even in this case, that y_2 does not exceed 350 K. Since the process is exothermic, system instability in terms of temperature can only emerge as overheating, which is addressed by the corollary. A similar corollary can be easily proven in the case that the concentration is intended to decline.

Two feedback control gains of -147.3616 and -0.0488 affect the temperature in the conditions presented in the corollary; the second one has no effect in the proof of the corollary, and the proof remains valid for any negative real number instead of −147.3616. This indicates the robustness of the control system against variation in feedback control gains.

Corollary. *Let us assume that the concentration is intended to increase, u_3 is limited between [280, 350] K, u_1 and u_2 are limited between [0, 60] L/min and y_{d2} is 350 K, then $\dot{y}_2 \leq 0$ at $y_2 = y_{d2} =$ 350 K.*

Proof. Equation (28) is the second equation in Equations (16) and (17):

$$\dot{y}_2(t) = \overbrace{u_1(t-0.1)(3.5-0.01y_2(t))}^{T1} + \overbrace{1.506\times10^{13}y_1(t)exp\left(\frac{-8750}{y_2(t)}\right)}^{T2}\overbrace{-2.092(y_2(t)-u_3(t-0.2))}^{T3}. \tag{28}$$

Evidently, $T1 = 0$ at $y_2 = 350$ K and $T1 < 0$ for temperatures higher than 350 K. In other words, $\dot{y}_2 \leq T2 + T3$. Thus, if

$$T2 + T3 \leq 0, \tag{29}$$

the corollary is proved. This leads to Equation (30) considering 4.2.4 or $y_2(t) \cong yp_2(t-0.2)$, where index p means predicted.

$$T3 = -2.092(y_2(t)-u_3(t-0.2)) = -2.092y_2(t) + 2.092u_3(t-0.2) \cong -2.092y_{p2}(t-0.2) + 2.092u_3(t-0.2). \tag{30}$$

Equations (20) and (25) and the corollary assumption of $y_{d2} = y_2 = 350$ K lead to Equation (31), where all times are $t-0.2$, and Section 4.2.4 is observed to assure synchrony.

$$u_3 = \left(-147.3616(y_{d1}-yp_1) - 7.2\times10^{12}y_{d1}exp\left(\frac{-8750}{y_{d2}}\right) + y_{d2}\right). \tag{31}$$

Equations (30) and (31) result in Equation (32):

$$T3 = -2.092y_{p2} + \left(-308.2805\left(y_{d1}-y_{p1}\right) - 1.506\times10^{13}y_{d1}exp\left(\frac{-8750}{y_{d2}}\right) + 2.092y_{d2}(t)\right). \tag{32}$$

Then $-2.092y_{p2} + (2.092y_{d2}) = 2.092\left(y_{d2}-y_{p2}\right) = 0$. Furthermore, as the concentration is intended to increase, $y_{d1} - y_{p1} > 0$, and, as a result, $-308.2805(y_{d1}-y_{p1}) < 0$ and $T3r \leq T3$, where $T3r$ is the remaining part of $T3$ without $-308.2805(y_{d1}-y_{p1})$ and $2.092\,(y_{d2}-y_{p2})$, presented in Equation (34). Evidently, $\dot{y}_2 \leq T2 + T3 \leq T2 + T3r$. Therefore, the condition of Equation (33) can replace Equation (29), or if

$$T2 + T3r \leq 0, \tag{33}$$

then the corollary is proven, where

$$T3r = -1.506\times10^{13}y_{d1}exp\left(\frac{-8750}{y_{d2}}\right). \tag{34}$$

With the use of Equations (28) and (34), the condition of Equation (33) can be presented as

$$\begin{aligned} T2 + T3r = \overbrace{1.506\times10^{13}-y_{p1}exp\left(\frac{-8750}{y_2(t)}\right)}^{T2}\overbrace{-1.506\times10^{13}y_{d1}exp\left(\frac{-8750}{y_{d2}}\right)}^{T3r} = \\ 1.506\times10^{13}exp\left(\tfrac{-8750}{y_{d2}}\right)(y_{p1}-y_{d1}) \leq 0. \end{aligned} \tag{35}$$

Evidently, $1.506 \times 10^{13} exp\left(\frac{-8750}{y_{d2}}\right) > 0$. Moreover, as the concentration is intended to increase, $y_{p1} - y_{d1} < 0$, or $y_{p1} - y_{d1} \leq 0$, if the concentration reference is touched too. Therefore, Equation (35) is true. □

4.2.6. Switching Remarks

Two models of Equations (14) and (15) are both equivalents of Equation (13) with q_w and q_f equal to zero, respectively. In other words, Equation (14) is Equation (13) when the concentration is intended to increase; thus, the water valve is closed or $q_w = u_2 = 0$, and Equation (15) is Equation (13) when the concentration is intended to decrease; hence, the feed valve is closed or $q_f = u_1 = 0$. Therefore, there is no real switching in system dynamics. However, the control laws in the aforementioned dual situations are different.

In terms of concentration control, an increase or decrease in the concentration is carried out with different actuators, a feed valve and water valve, respectively. As a result, switching, in its usual form, does not occur, because the control law of each actuator remains unchanged. Equation (20) only works on u_1 and Equation (21) on u_2. The feedforward control law is the same when the concentration is intended to increase or decrease. In other words, the water valve simply turns OFF when the concentration error becomes negative, i.e., the concentration is smaller than its reference and needs to increase, and the feed valve turns OFF when the concentration error becomes positive, or the concentration exceeds its reference.

In temperature control, the single main input is the temperature of auxiliary flow, u_3, and switching occurs when the control law changes. However, at the point of switching, where concentration error is zero or $y_{d1} = y_1$, both Equations (20) and (21) lead to the same control law of Equation (36):

$$u_3 = -0.0488(y_{d2} - y_2) + u^*{}_3. \tag{36}$$

Therefore, there will be no sudden change in control input at the point of switching. Please note that Equations (20), (21) and (36) are valid for a delay-free system. In order to consider the time delays, Section 4.2.4 and prediction, predicted outputs y_{p1} and y_{p2} should replace y_1 and y_2.

5. Results and Discussion

Figures 4 and 5 compare the simulation results of the proposed enhanced SPCS with a conventional SPCS with two arrays of PIDs, four each, carefully turned for the delay-less form of transfer functions in Equations (26) and (27), as detailed in the Appendix A. PIDs are still the dominant controller for SPCSs [39–41]. A conventional SPCS was also designed for the case study with PIDs tuned using decentralized and centralized multivariable approaches. However, it failed to exhibit a presentable performance showing the challenging nature of this control problem. The original nonlinear system of Equation (13) has been used in simulations with a sampling frequency of 1 Hz, which is easily achievable in practice. The range of auxiliary temperatures is [280, 350] K, and the maximum flow rate of valves is 60 L/min. No measurement noise was considered in the simulations presented in Figures 4 and 5.

The enhanced SPCS evidently outperforms conventional SPCS with PIDs in concentration control and catches the temperature reference much faster. The results also show that changes in the concentration reference affect the temperature control for the proposed control system. The reason is that the proposed control system prioritizes concentration control, as a design requirement, through the selection of a faster closed-loop pole for the concentration. Interestingly, the upper graph of Figure 5 shows that the proposed control system uses the capacity of valves in full to compensate for the error where the reference changes. The conventional SPCS with PIDs does not use this capacity and is consequently slower. This behaviour is rooted in the inherent trade-off in the PID design that slows down the system to avoid concentration overshoots. Moreover, the effect of integral windup is evident in the bottom graph of Figure 5 as another weak point of the conventional SPCS with PIDs. These are the same shortcomings predicted in Section 3, addressed with the proposed Enhancement 1.

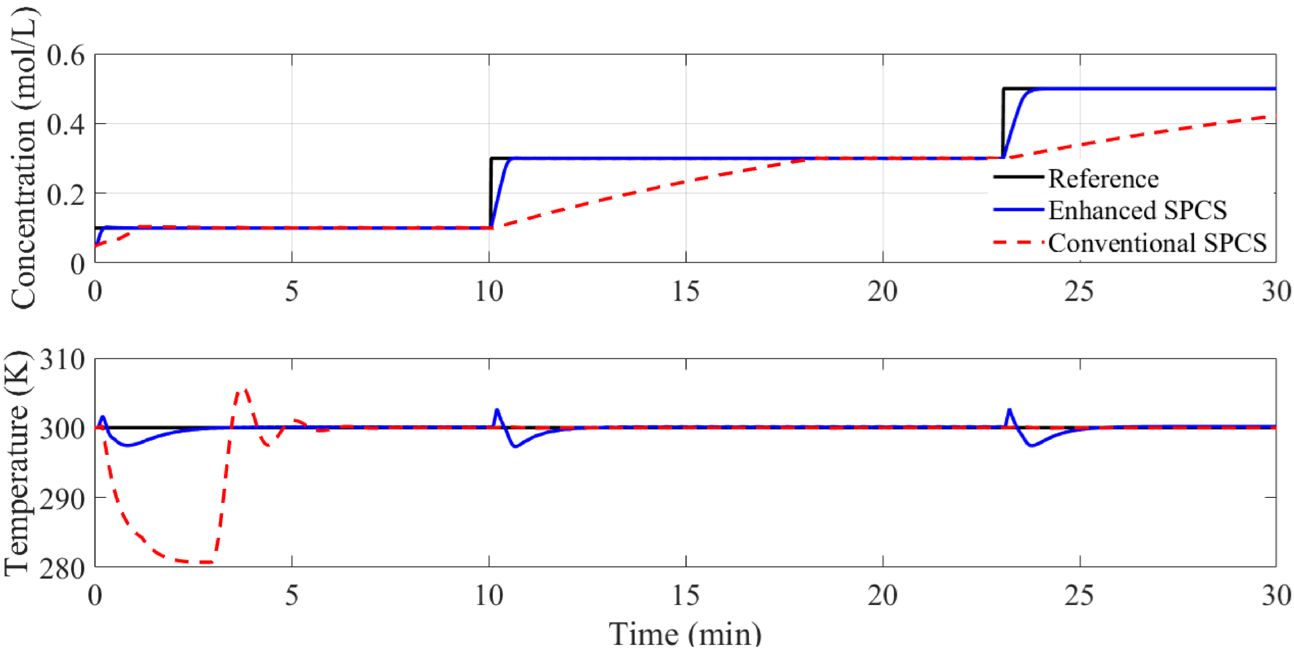

Figure 4. Control outputs for conventional SPCS with PIDs and the enhanced SPCS, without noise.

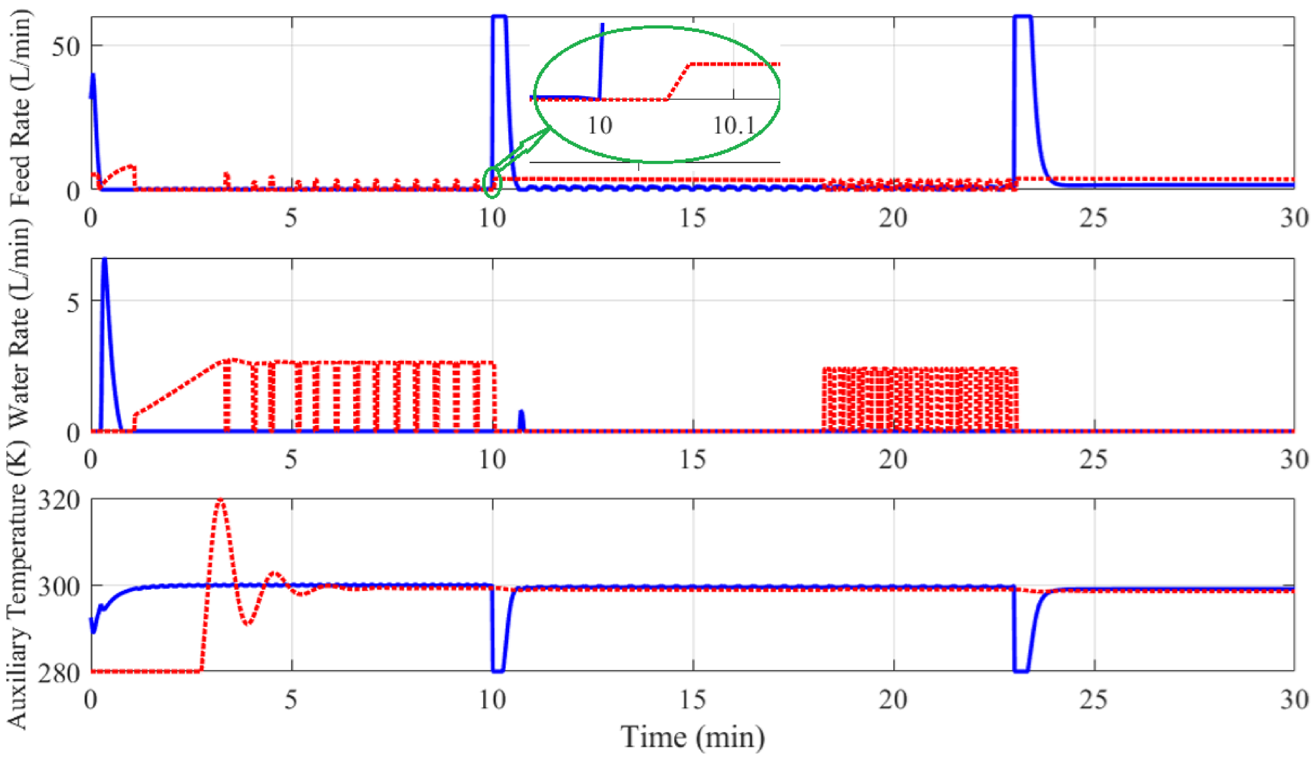

Figure 5. Control inputs for conventional SPCS with PIDs and enhanced SPCS without noise, related to control outputs presented in Figure 4.

Figure 5 also indicates that, in the proposed control system, significant and fast changes in control inputs only occurred at the beginning of operation or in the case of a change in the reference, while a conventional SPCS with PIDs turns water/feed valves ON/OFF very frequently, e.g., in time periods of 3–10 min and 18–23 min, and struggles to maintain the concentration based on the reference, after it is reached. This is a great advantage for the proposed enhanced SPCS in terms of implementation and energy consumption. This advantage is influenced by the feedforward component of the enhanced SPCS, proposed by Enhancement 1. In order to elucidate such an influence, it should be noted that the CSTR (like many other processes) matches the definition of the generalized type zero (GTZ) systems proposed in [57]. In a GTZ system, the control equilibrium point (CEP) of the system is maintained only via continuous exertion of a control input; CEP is the situation where the error and its derivatives are zero [58]. The feedforward component in Equation (8), u_j^*, suggested in the proposed Enhancement 1 and detailed in Equation (25) for the case study, has been designed to maintain the desired status of Equation (10), when it is reached. The desired status equals CEP in the case study of this paper, as detailed in Section 4.2.2. In the absence of Enhancement 1 and such a feedforward component, in the control systems merely relying on feedback controllers, when the reference is reached, the control input drops to zero shortly, which cannot keep a GTZ on the reference; this leads to a rise in the error and a jump in the control input to compensate for it, e.g., the jumps in the middle graph of Figure 5.

The area outlined with an ellipse in Figure 5 shows the effect of Enhancement 2, where output of the Smith predictors is compared with its asynchronous value of reference in the future to produce the predicted error; please note that the reference changes at 10.05 min or 10 min and 3 s, not exactly at 10 min. The predicted error is fed into Equations (20) or (21) for timely action and improved performance.

Figure 6 is similar to Figure 4 but with an addition: the influence of random measurement noises of ±0.4 K and ±2% for the temperature and concentration, respectively. Such noises are considered moderate for the case study [59,60]. Both control systems can handle noises very well.

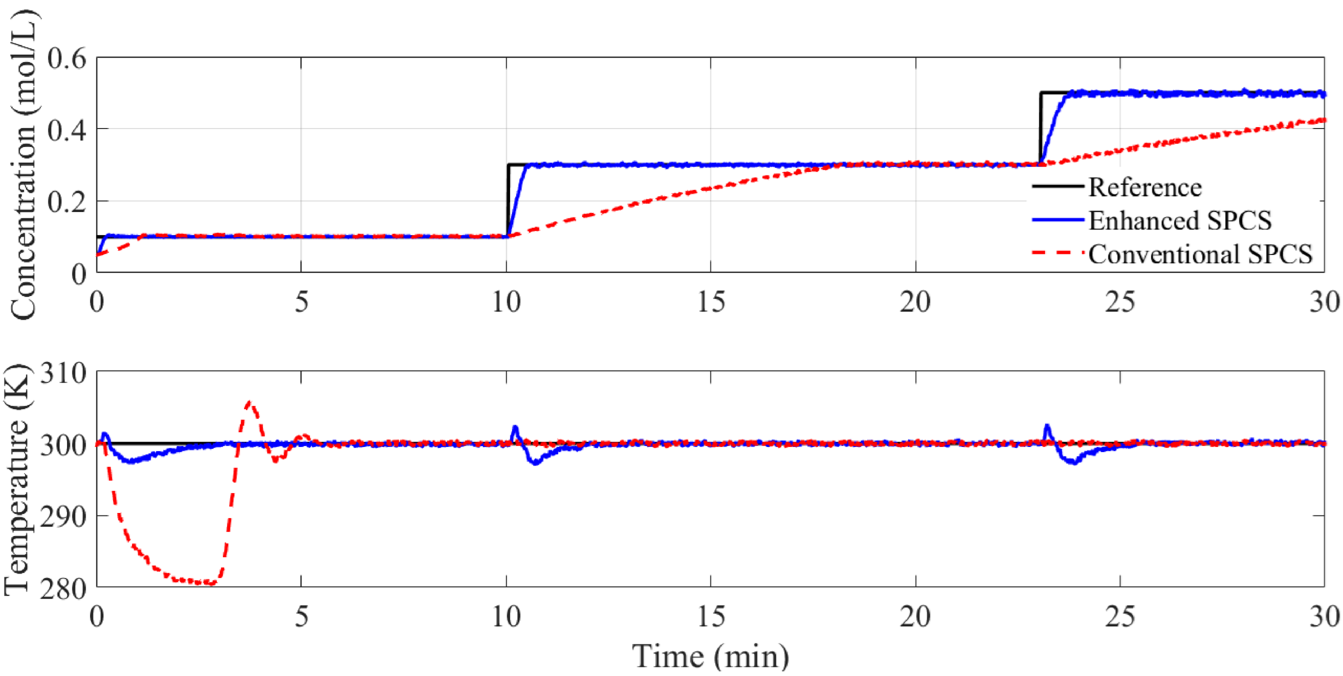

Figure 6. Simulation results with the proposed control system and conventional SPCS with PIDs. Noises are added.

In order to assess the sensitivity of the control system to the accurate estimation of model parameters, some noise-free simulations were carried out, all with the reference shown in Figures 4–6. In these simulations, control commands of u_1 and u_3 are multiplied by a variety of coefficients close to 1, u_2 is mostly zero as the concentration is not intended to decrease. The discrepancy in these coefficients with 1 represents errors in estimation of the right control command due to model uncertainties, through errors both in the identification of control law parameters and development of Smith predictor models of Equations (26) and (27). Results are presented in Table 2. It is evident that the concentration, y_1, control performance is not hurt with a change in the coefficients, while the temperature, y_2, is quite sensitive to u_3. It may be rooted in the design process that prioritizes the concentration.

Table 2. Mean of absolute error and maximum overshoot in the proposed enhanced SPCS when control commands are multiplied by different coefficients.

	u_1 Coefficient	u_3 Coefficient	MAE (Mean of Absolute Error)	Maximum Overshoot
y_1 [mol/L]	1	1	0.0038	0.0027
y_2 [K]			0.3536	2.7297
y_1 [mol/L]	08	1	0.0041	0.0004
y_2 [K]			0.3594	2.7092
y_1 [mol/L]	1.2	1	0.0038	0.0061
y_2 [K]			0.3454	2.7439
y_1 [mol/L]	0.9	0.9	0.0038	0.0014
y_2 [K]			18.8041	1.4843

6. Conclusions

In this paper, initially, two shortcomings of conventional Smith-predictor-based control systems for MIMO time-delay processes were identified: (i) the use of classical feedback controllers with their inherent limitations and (ii) asynchrony between the reference and the predicted output. The latter particularly causes the response to lag behind the reference. Accordingly, two enhancements were proposed for SPCSs designed for MIMO time-delay processes: (i) replacing the array of classical feedback controllers with a feedback–feedforward arrangement, and (ii) providing the control system with some future reference value(s) upfront. Section 3 presents the proposed control system in depth.

The proposed enhanced SPCS was examined to control a nonlinear exothermic MIMO CSTR with multiple time delays and demonstrated clear superiority over a conventional SPCS with PID feedback controllers. The employed CSTR model incorporates an exceptional level of details and thoroughness in terms of inputs, outputs, time-delays, actuators' limitations and sensor noises, thereby ensuring that the results are realistic and the proposed method is implementable. The proposed method not only presented excellent tracking performance, but also, it witnessed much fewer undesirable rapid changes of control inputs.

Author Contributions: Conceptualization, M.M. and G.V.-N.; Methodology, M.M. and A.A.; Investigation, A.A.; Resources, M.M. and M.G.; Writing—original draft, M.M. and A.A.-H.; Writing—review and editing, M.M., G.V.-N., A.A., M.G. and P.S.; Project administration, A.A.-H.; Funding acquisition, A.A.-H. All authors have read and agreed to the published version of the manuscript.

Funding: Research reported in this paper was supported by the German University of Technology in Oman, through Seed Grant #SG2025/NR/ENG/MM.

Data Availability Statement: The original contributions presented in this study are included in the article. Further inquiries can be directed to the corresponding authors.

Conflicts of Interest: The authors declare no conflicts of interest.

Nomenclature

BW	bandwidth
CEP	control equilibrium point
CSTR	catalytic stirred tank reactor
GTZ	generalized type zero
MIMO	multi-input multi-output
PID	proportional integral derivative
PM	phase margin
SISO	single-input single-output
Latin Letters	
c	specific heat coefficient [g/(L.K)]
C	concentration [mol/L]
$C(s)$	controller transfer function
$G(s)$	plant transfer function
e	control error
E	Arrhenius activation energy [J/mol]
H	heat of reaction [J/min]
k	counting index
n	number
P	pole
q	flow rate [L/min]
r	discrete delay
R	gas constant [J/(mol.K)]
s	Laplace variable
t	time/ time delay without/with an index
T	temperature [K]
u	control input
V	reactor volume [L]
x	system state
y	output
z	Z-transform variable
Vectors and Matrices	
$\mathbf{A}$	system matrix
$\mathbf{B}$	input matrix
$\mathbf{C}$	output matrix
$\mathbf{K}$	controller gain matrix
$\mathbf{U}$	control input vector
$\mathbf{X}$	state vector
$\mathbf{Y}$	output vector
Subscripts	
A	effluent
d	desired
f	feed
i,j	index
p	predicted
s	sampling
u	related to input
w	water

x	auxiliary
y	related to output
Superscripts	
*	related to the desired status
ˆ	approximated
Greek Letters	
β	gain of a first order transfer function
κ	reaction velocity constant [min^{-1}]
ρ	*density* [g/L]
τ	time constant of a first order transfer function
ι	index

Appendix A. PID Tuning for Conventional SPCS

The pidtune command of MATLAB Control System Toolbox, version 24.2, was used in this research to tune PIDs for the conventional SPCS of Equation (5) [61], where centralized and decentralized MIMO tuning of PIDs led to extremely poor tracking performance and practically failed. The PID of $C(s)$ is tuned for the plant of $G(s)$:

$$C(s) = K_P + \frac{K_I}{s} + K_D s, \tag{A1}$$

In the employed algorithm, a target crossover frequency, ω_c, and PID controller parameters, K_P, K_I and K_D are picked; then, the condition of Equation (A2) and suitability of bandwidth, BW, in Equation (A5), maximum sensitivity in Equation (A4) and phase margin, PM in Equation (A3), are checked. Afterwards, the target crossover frequency and PID parameters are numerically tuned in an iterative fashion until Equation (A2) is met and Equations (A3)–(A5) lead to suitable values.

$$|C(j\omega_c)G(j\omega_c)| = 1, \tag{A2}$$

$$\mathrm{PM} = 120^\circ + \angle C(j\omega_c) + \angle G(j\omega_c), \tag{A3}$$

$$\text{Maximin Sensitivity} = max\left|\frac{1}{1 + C(j\omega_c)G(j\omega_c)}\right|, \tag{A4}$$

$$\mathrm{BW} = \left\{\omega : \left|\frac{C(j\omega)G(j\omega)}{1 + C(j\omega)G(j\omega)}\right| = 0.707\right\}. \tag{A5}$$

In Table A1, $C_{I\ or\ D}ij$ is a PID that connects input j to output i. Index I or D mean the concentration is intended to increase or decrease, respectively.

Table A1. Parameters of different PIDs used to form an alternative to the proposed enhanced SPCS.

Controller	K_P	K_I	K_D
C_I 11	2.82	0.08	0
C_I21	0.50	0.06	0
C_I 13	0	−1	0
C_I 23	1.58	6.02	0
C_D 12	−11.3	0.32	0
C_D 22	0	0.05	0
C_D 13	0	−1	0
C_D 23	1.58	6.02	0

References

1. Li, X.; Liu, W.; Gorbachev, S.; Cao, J. Event-triggered impulsive control for input-to-state stabilization of nonlinear time-delay systems. *IEEE Trans. Cybern.* **2023**, *54*, 2536–2544. [CrossRef] [PubMed]
2. Sharma, S.; Padhy, P.K. An indirect approach for online identification of continuous time-delay systems. *Int. J. Numer. Model. Electron. Netw. Devices Fields* **2022**, *35*, e2947. [CrossRef]
3. Huba, M.; Bistak, P.; Vrancic, D.; Sun, M. PID vs. Model-Based Control for the Double Integrator Plus Dead-Time Model: Noise Attenuation and Robustness Aspects. *Mathematics* **2025**, *13*, 664. [CrossRef]
4. Sharma, P.; Neeli, S. A systematic review of discretisation methods for time-delay systems. *J. Control Decis.* **2025**, *12*, 335–350. [CrossRef]
5. Abdusalomov, A.; Khusanov, S.; Ibragimov, I.; Sevinov, J.; Mukhiddinov, M.; Cho, Y.I. Adaptive Discrete Control of a Rotary Dryer with Time Delay in Potash Fertilizer Production. *Processes* **2026**, *14*, 871. [CrossRef]
6. Liu, Z.-G.; Jiang, Z.-W.; Sun, W.; Su, S.-F. Decentralized Tracking Control of Large-Scale Time-Delay Nonlinear Systems and Application to Chemical Reactor System. *IEEE Trans. Syst. Man Cybern. Syst.* **2025**, *55*, 5553–5564. [CrossRef]
7. Liu, P.-L. Further results on delay-range-dependent stability with additive time-varying delay systems. *ISA Trans.* **2014**, *53*, 258–266. [CrossRef] [PubMed]
8. Araújo, J.M.; Santos, T.L.M. Control of a class of second-order linear vibrating systems with time-delay: Smith predictor approach. *Mech. Syst. Signal Process.* **2018**, *108*, 173–187. [CrossRef]
9. Vazquez Guerra, R.J.; Marquez Rubio, J.F.; del Muro-Cúellar, B. Design of delayed PID-type controllers for high-order recycling systems with time delays using model reduction. *Asia-Pac. J. Chem. Eng.* **2021**, *16*, e2670. [CrossRef]
10. Korupu, V.L.; Muthukumarasamy, M. A comparative study of various Smith predictor configurations for industrial delay processes. *Chem. Prod. Process Model.* **2021**, *17*, 701–732. [CrossRef]
11. Mohammadzaheri, M.; Ghodsi, M. An Enhanced Smith-Predictor-based Control System for delayed MIMO Processes and its Use on a CSTR with Multiple Time-delays. In *Proceedings of the 2023 28th International Conference on Automation and Computing (ICAC), Birmingham, UK, 30 August–1 September 2023*; IEEE: New York, NY, USA, 2023; pp. 1–6.
12. Chen, H.; Li, Q.; Ye, Z.; Pang, S. Neural Network-Based Parameter Estimation and Compensation Control for Time-Delay Servo System of Aeroengine. *Aerospace* **2025**, *12*, 64. [CrossRef]
13. Kumari, P.; Kumar, P.; Ali, M.H.; Manikanta, G.; Pandey, A.K.; Saha, A.K. Nonlinear Active Disturbance Rejection Control for Unstable Processes with Time Delay: A Case Study of a Continuous Stirred Tank Reactor. *Results Eng.* **2026**, *30*, 110296. [CrossRef]
14. Li, X.; de Souza, C.E. Delay-dependent robust stability and stabilization of uncertain linear delay systems: A linear matrix inequality approach. *IEEE Trans. Autom. Control* **1997**, *42*, 1144–1148. (In English) [CrossRef]
15. Ri, K.-C.; Kim, Y.-I.; Ri, S.-J. Robust fault-tolerant control and application in DCS with uncertainty and time delay. *Int. J. Dyn. Control* **2025**, *13*, 44. [CrossRef]
16. Phan, V.D.; Mai, T.A.; Ho, S.P.; Dang, T.S.; Le, V.C.; Dinh, V.N. Development of an adaptive integral terminal sliding mode tracking control for a wheeled mobile robot with time delay estimation. *Int. J. Control Autom. Syst.* **2025**, *23*, 2399–2410. [CrossRef]
17. Mohammadzaheri, M.; Tafreshi, R. An enhanced Smith predictor based control system using feedback-feedforward structure for time-delay processes. *J. Eng. Res.* **2017**, *14*, 156–165. [CrossRef]
18. Li, H.; Song, B.; Wang, S.; Shi, H.; Li, P. Robust safety predictive tracking control for batch processes: Deception attacks in unreliable network channels. *Comput. Chem. Eng.* **2026**, *210*, 109642. [CrossRef]
19. Wu, M.; He, Y.; She, J.H. *Stability Analysis and Robust Control of Time-Delay Systems*; Springer: Berlin/Heidelberg, Germany, 2010.
20. Zhi, Y.-L.; Liu, X.; He, S.; Lin, W.; Chen, W. Adaptively Event-Triggered H∞ Control for Networked Autonomous Aerial Vehicles Control Systems Under Deception Attacks. *IEEE Trans. Ind. Inform.* **2025**, *21*, 3458–3465. [CrossRef]
21. Zhong, Q.C. *Robust Control of Time-Delay Systems (No. 2009)*; Springer: Berlin/Heidelberg, Germany, 2006.
22. Cai, J.; Guo, D.; Wang, W. Adaptive fault-tolerant control of uncertain systems with unknown actuator failures and input delay. *Meas. Control* **2025**, *58*, 923–934. [CrossRef]
23. Divakar, K.; Kumar, M.P.; Dhanamjayulu, C.; Gokulakrishnan, G. A Technical Review on IMC-PID Design for Integrating Process with Dead Time. *IEEE Access* **2024**, *12*, 124845–124870. [CrossRef]
24. Bequette, B.W. *Process Control: Modeling, Design, and Simulation*, 2nd ed.; Prentice Hall Professional: Hoboken, NJ, USA, 2023.
25. Mohammadzahri, M.; Khaleghifar, A.; Ghodsi, M.; Soltani, P.; AlSulti, S. A Discrete Approach to Feedback Linearization, Yaw Control of An Unmanned Helicopter. *Unmanned Syst.* **2023**, *11*, 57–66. [CrossRef]
26. Mohammadzaheri, M.; Al-Humairi, A.; Vakili-Nezhaad, G.; Jones, A.A.S.; Hamlin, C.; Ghodsi, M.; Soltani, P. Digital Model-Based Motor Servo Control Considering a Sampling-Induced Time Delay. In *Proceedings of the 12th International Conference on Control, Dynamic Systems, and Robotics, CDSR 2025, London, UK, 13–15 July 2025*; Avestia Publishing: Ottawa, ON, Canada, 2025; p. 9.
27. Perev, K. Feedback control for plants with time delay. In *IOP Conference Series: Materials Science and Engineering*; IOP Publishing: Bristol, UK, 2024; Volume 1317, p. 012002.
28. Smith, O.J. Closer control of loops with dead time. *Chem. Eng. Prog.* **1957**, *53*, 217–219.

29. Santos, T.L.; Flesch, R.C.; Normey-Rico, J.E. On the filtered Smith predictor for MIMO processes with multiple time delays. *J. Process Control* **2014**, *24*, 383–400. [CrossRef]
30. Azarmi, R.; Sedigh, A.K.; Tavakoli-Kakhki, M.; Fatehi, A. Design and implementation of smith predictor based fractional order PID controller on MIMO flow-level plant. In *Proceedings of the 23rd Iranian Conference on Electrical Engineering, Tehran, Iran, 10–14 May 2015*; IEEE: New York, NY, USA, 2015; pp. 858–863.
31. Dogruer, T. Design of I-PD controller based modified smith predictor for processes with inverse response and time delay using equilibrium optimizer. *IEEE Access* **2023**, *11*, 14636–14646. [CrossRef]
32. Astrom, K.J.; Hang, C.C.; Lim, B. A new Smith predictor for controlling a process with an integrator and long dead-time. *IEEE Trans. Autom. Control* **1994**, *39*, 343–345. [CrossRef]
33. Mehallel, A.; Feliu-Batlle, V. Reduction of the Disturbance Effects in a Twin Rotor Multi-Input Multi-Output System Based on a Modified Smith Predictor Control Scheme. *Appl. Sci.* **2025**, *15*, 5499. [CrossRef]
34. DePoar, A. A modified Smith predictor and controller for unstable processes with time delay. *Int. J. Control* **1985**, *41*, 1025–1036. [CrossRef]
35. Albertos, P.; Luan, X.; Garcia, P. Smith predictor based control of multi time-delay processes. *Annu. Rev. Control* **2025**, *60*, 101008. [CrossRef]
36. Ebrahimi, B.; Tafreshi, R.; Mohammadpour, J.; Franchek, M.; Grigoriadis, K.; Masudi, H. Second-Order Sliding Mode Strategy for Air--Fuel Ratio Control of Lean-Burn SI Engines. *IEEE Trans. Control Syst. Technol.* **2014**, *22*, 1374–1384. [CrossRef]
37. Ebrahimi, B.; Tafreshi, R.; Franchek, M.; Grigoriadis, K.; Mohammadpour, J. A dynamic feedback control strategy for control loops with time-varying delay. *Int. J. Control* **2014**, *87*, 887–897. (In English) [CrossRef]
38. Ogunnaike, B.; Ray, W. Multivariable controller design for linear systems having multiple time delays. *AIChE J.* **1979**, *25*, 1043–1057. [CrossRef]
39. Pataro, I.M.; da Costa, M.V.A.; Joseph, B. Advanced Simulation and Analysis of MIMO Dead Time Compensator and Predictive Controller for Ethanol Distillation Process. *IFAC-PapersOnLine* **2019**, *52*, 160–165. [CrossRef]
40. Guo, X.; Shirkhani, M.; Ahmed, E.M. Machine-Learning-Based improved smith predictive control for MIMO processes. *Mathematics* **2022**, *10*, 3696. [CrossRef]
41. Singha, P.; Meena, R.; Chakraborty, S.; Raja, G.L. Robust pidf-pid cascade control scheme for delay-dominant stable and integrating chemical processes. *J. Taiwan Inst. Chem. Eng.* **2025**, *173*, 106165. [CrossRef]
42. Aryan, P.; Mohammadzaheri, M.; Chen, L.; Ghanbari, M.; Mirsepahi, A. GA-IMC based PID control design for an infrared dryer. In Proceedings of the Chemeca, Adelaide, South Australia, 26–29 September 2010.
43. Asadi, F. *State-Space Control Systems: The MATLAB®/Simulink® Approach*; Springer Nature: Berlin/Heidelberg, Germany, 2022.
44. Li, L.; Liao, F. Parameter-dependent preview control with robust tracking performance. *IET Control Theory Appl.* **2017**, *11*, 38–46. [CrossRef]
45. Birla, N.; Swarup, A. Optimal preview control: A review. *Optim. Control Appl. Methods* **2015**, *36*, 241–268. [CrossRef]
46. Na, J.; Ren, X.; Shang, C.; Guo, Y. Adaptive neural network predictive control for nonlinear pure feedback systems with input delay. *J. Process Control* **2012**, *22*, 194–206. [CrossRef]
47. Mohammadzaheri, M.; Chen, L. Double-command feedforward-feedback control of a nonlinear plant. *Korean J. Chem. Eng.* **2010**, *27*, 1372–1376. (In English) [CrossRef]
48. Sistu, P.B.; Bequette, B.W. A comparison of nonlinear control techniques for continuous stirred tank reactors. *Chem. Eng. Sci.* **1992**, *47*, 2553–2558. [CrossRef]
49. Alvarez-Ramirez, J.; Femat, R. Robust PI stabilization of a class of chemical reactors. *Syst. Control Lett.* **1999**, *38*, 219–225. [CrossRef]
50. Ghaffari, V.; Naghavi, S.V.; Safavi, A. Robust model predictive control of a class of uncertain nonlinear systems with application to typical CSTR problems. *J. Process Control* **2013**, *23*, 493–499. [CrossRef]
51. Kuntanapreeda, S.; Marusak, P.M. Nonlinear extended output feedback control for CSTRs with van de Vusse reaction. *Comput. Chem. Eng.* **2012**, *41*, 10–23. [CrossRef]
52. Mohammadzaheri, M.; Chen, L. Double-command fuzzy control of a nonlinear CSTR. *Korean J. Chem. Eng.* **2010**, *27*, 19–31. [CrossRef]
53. Pérez, M.; Albertos, P. Self-oscillating and chaotic behaviour of a PI-controlled CSTR with control valve saturation. *J. Process Control* **2004**, *14*, 51–59. [CrossRef]
54. Sukkarnkha, P.; Panjapornpon, C. Input/output linearization with a two-degree-of-freedom scheme for uncertain nonlinear processes. *Korean J. Chem. Eng.* **2012**, *29*, 716–723. [CrossRef]
55. ZareNezhad, B.; Aminian, A. Application of the neural network-based model predictive controllers in nonlinear industrial systems. Case study. *J. Univ. Chem. Technol. Metall.* **2011**, *46*, 67–74.

56. Izci, D.; Ekinci, S.; Ökten, I.; Çınar, R.F.; Rashdan, M.; Salman, M.; Güneş, B.B.; Ahmad, M.A. A novel hyperbolic tangent-augmented controller framework for temperature control in jacketed continuous stirred tank reactors. *Sci. Rep.* **2026**, *16*, 16661. [CrossRef] [PubMed]
57. Mohammadzaheri, M.; Chen, L.; Mirsepahi, A.; Ghanbari, M.; Tafreshi, R. Neuro-Predictive Control of an Infrared Dryer with a Feedforward-Feedback Approach. *Asian J. Control* **2015**, *17*, 1972–1977. [CrossRef]
58. Mohammadzaheri, M.; Chen, L. Design and stability discussion of an hybrid intelligent controller for an unordinary system. *Asian J. Control* **2009**, *11*, 476–488. [CrossRef]
59. Pearce, A.N.; Bojkovski, J.; Edler, J.; de Groot, F.; Izquierdo, M.; Kalemci, G.G.; Strnad, M. "Guidelines on the Calibration of Thermocouples," Good Practice Guide 2020. Available online: https://www.euramet.org/publications-media-centre/calibration-guidelines/ (accessed on 22 January 2026).
60. Gorla, G.; Iturrioz, J.A.; Esbensen, K.H.; Amigo, J.M. Getting "sampling" right for reliable process monitoring: Main challenges and solutions. *Front. Anal. Sci.* **2026**, *6*, 1839552. [CrossRef]
61. MathWorks. Pidtune. Available online: https://www.mathworks.com/help/control/ref/dynamicsystem.pidtune.html (accessed on 22 January 2026).